



# Ordered adsorption of ketones on Cu(6 4 3) revealed by scanning tunneling microscopy

Xueying Zhao, Scott S. Perry\*

Department of Chemistry, University of Houston, 4800 Calhoun Road, Houston, TX 77204-5003, USA

## Abstract

Adsorption of three ketones, *R*-3-methyl-cyclohexanone, cyclohexanone, and 2-hexanone, on the chiral Cu(6 4 3) surface has been investigated with scanning tunneling microscopy (STM) under ultrahigh vacuum conditions. The measurements reveal that the clean Cu(6 4 3) surface is composed of a well-ordered and evenly spaced step and terrace structure. In addition, the measurements indicate a high mobility of Cu atoms along the steps of the surface held at room temperature. Upon adsorption at room temperature, all the three ketones form ordered structures on Cu(6 4 3) consisting of one molecule per terrace width with a spacing along the step direction commensurate with the ideal kink spacing. The ordered structures of cyclohexanone are consistent with the reconstruction of the Cu(6 4 3) to a surface composed of (11 7 5) (major) and (5 3 2) (minor) facets. This reconstruction comprises an effective reduction in terrace width while preserving the kinked step structure.  
© 2004 Published by Elsevier B.V.

**Keywords:** Copper; Chiral surface; High Miller index; Scanning tunneling microscopy

## 1. Introduction

Although metal single-crystals themselves are achiral, certain crystallographic orientations of their surfaces are inherently chiral. Recent investigations both in theoretical calculations [1–3] and in experiments [4–7] have confirmed that intrinsic chiral metal surfaces exhibit enantiospecific properties. For example, theoretical simulations carried out by Sholl have predicted a more than 2 kcal/mol difference in the adsorption energies of the enantiomers of limonene when adsorbed on the chiral Pt(6 4 3) and Pt(5 3 2) surfaces [2]. Experimentally, the electro-oxidation of *D*- and *L*-glucose on the chiral electrodes *R*- and *S*-Pt(6 4 3) investigated by Attard et al. has demonstrated that both electrodes are enantioselective [4]. In addition, Gellman et al. have observed in temperature programmed desorption (TPD) measurements that the desorption energies of *R*-3-methyl-cyclohexanone (*R*-3-MCHO) differ by  $0.22 \pm 0.05$  kcal/mol on the *R*- and *S*-Cu(6 4 3) surfaces [6,7]. While these studies have demonstrated the chiral behavior of these surfaces, little is known of the local details of adsorption on such chiral surfaces.

Inspired by these results, we have used scanning tunneling microscopy (STM) to observe the surface structure of the highly stepped single-crystal copper surfaces Cu(6 4 3), before and after adsorption of the chiral ketone molecule (*R*-3-MCHO) as well as two other achiral ketones: cyclohexanone and 2-hexanone. For *R*-3-MCHO and 2-hexanone, we find that adsorbed overlayers of these molecules possess features commensurate with the ideal structure of the Cu(6 4 3) surface, despite the high mobility of Cu atoms at room temperature along step edges. The adsorption of cyclohexanone leads to similar overlayer structures, however the STM results indicate a restructuring of the Cu(6 4 3) surface involving a reduction in terrace width but a preservation of the kinked step structure. While the results presented here do not directly reveal the origin of the enantiospecific properties of the *R*-3-MCHO/Cu(6 4 3) interaction observed by Gellman et al., they do provide the first direct evidence of the spatial orientation of molecules on highly stepped, chiral transition metal surfaces and illustrate the influence of adsorbate molecular structure on the stability of such surfaces.

## 2. Experimental

Experiments were conducted with an Omicron STM system housed in a vacuum chamber with a base pressure less

\* Corresponding author. Tel.: +1-713-743-2715; fax: +1-713-743-2709.

E-mail address: [perry@uh.edu](mailto:perry@uh.edu) (S.S. Perry).

than  $1 \times 10^{-10}$  Torr. The copper crystal sample was purchased from Monocrystal Co. with a purity of more than 99.999%. The three ketones, *R*-3-MCHO, cyclohexanone, and 2-hexanone were purchased from Aldrich Co. with a purity of 98%. Prior to introduction to the vacuum chamber, the ketones were subjected to several freeze–pump–thaw cycles. The copper sample was cleaned in the vacuum chamber by cycles of 1.25 keV Ar<sup>+</sup> ion sputtering, while annealing to 1000 K until clear low energy electron diffraction (LEED) patterns appeared. Ketone exposure was carried out by back-filling the chamber through a variable leak valve at fixed pressures and predetermined time periods. STM tips were prepared from 0.2 mm diameter tungsten wires by etching in 2 M NaOH solution. In these experiments, a bias voltage was applied to the sample and STM images were obtained in a topography mode with a tip scan rate of  $\sim 20$ – $200$  nm/s. The specific tunneling conditions for the various images are reported in the relevant figure captions.

### 3. Results and discussion

#### 3.1. The clean Cu(643) surface

The bulk terminated Cu(643) surface is composed of (111) terraces separated by equidistant kinked monatomic steps (Fig. 1a). Following the cleaning procedure described above, we obtained LEED patterns (not shown) of the Cu(643) surface consistent with this structure and the images previously reported by Gellman et al. [7]. The basic features of the LEED pattern comprise a set of split diffraction spots in a hexagonal array, as expected. The splitting direction of spots indicates that the steps are oriented in real space  $\sim 19^\circ$  away from the [110] close-packed direction (Fig. 1a). Furthermore, the clear separation of split spots indicates that steps are arrayed on average in an equidistant manner on the clean surface.

The structure of the stepped surface was confirmed in STM images of the clean Cu(643) surface as well. A

representative image of a  $100 \text{ \AA} \times 100 \text{ \AA}$  area is shown in Fig. 1b and illustrates the terraced nature of the surface structure as well as the atomic structure within the terraces. From these images, although the steps appeared streaked, the average step height could be measured and corresponded to the ideal single step height ( $2.1 \text{ \AA}$ ). The average terrace width in these images is  $7.8 \pm 0.3 \text{ \AA}$ —measured simply as the distance between vectors drawn along average step directions—which falls within experimental error of the ideal value of  $7.55 \text{ \AA}$  ( $d_2 \sin \theta$ , Table 1). The streaked appearance of the steps in the STM image collected at room temperature results from a high mobility of copper atoms along the steps edges. Similar observations have been previously reported in STM studies of other vicinal copper surfaces [8–10].

#### 3.2. Adsorption of *R*-3-methyl-cyclohexanone on Cu(643)

Fig. 2 displays STM images obtained from the *R*-Cu(643) surface after being dosed with  $\sim 20$  L of *R*-3-MCHO at room temperature. It was found that *R*-3-MCHO forms an ordered adsorption structure on Cu(643) at room temperature under UHV conditions. Within the overlayer structure, individual molecules of *R*-3-MCHO appear as singular regions of high tunneling current under the conditions employed, with rows of these features oriented in a direction along the theoretical step edge direction. Within these rows, the average adsorbate–adsorbate spacing ( $d_1$ ) along the step direction is  $6.8 \pm 0.1 \text{ \AA}$ , identical to the theoretical distance between kink sites along steps of an ideal (643) surface (Table 1). Upon closer inspection of Fig. 2b, it is noted that a few minor domains within the adsorbate structure exist, which can be correlated to variations in kink site separations along the step as well as in the alignment of kink sites within neighboring steps.

Although direct evidence of the exact adsorption geometry of *R*-3-MCHO on Cu(643) is not provided through the STM images, we propose that *R*-3-MCHO adopts an orientation with the ring roughly parallel to the (111) terraces.

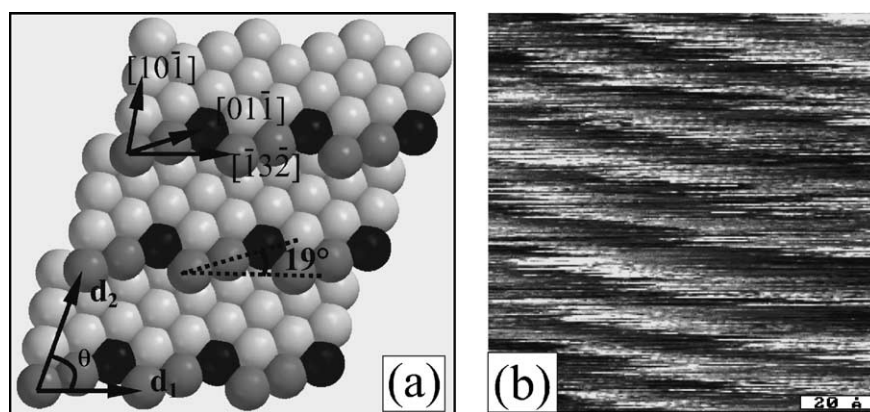


Fig. 1. (a) Model structure of chiral copper surface: *R*-Cu(643). The surface is composed of arrays of equidistant kinked steps separated by narrow (111) terraces. Step atoms are highlighted in dark gray while atoms at the apex of a kink are highlighted in black. (b) STM image obtained on clean Cu(643) at room temperature under the conditions:  $100 \text{ \AA} \times 100 \text{ \AA}$ ,  $-1.0$  V bias,  $0.7$  nA tunneling current.

Table 1

Lattice unit cell parameters for ketone adsorption overlayers on Cu(643), as well as on induced facets

| Adsorbate/substrate    | Theoretical |             |                | Experimental  |               |              |
|------------------------|-------------|-------------|----------------|---------------|---------------|--------------|
|                        | $d_1^a$ (Å) | $d_2^a$ (Å) | $\theta^a$ (°) | $d_1$ (Å)     | $d_2$ (Å)     | $\theta$ (°) |
| Cu/(643)               | 6.76        | 8.08        | 69.1           | –             | –             | –            |
| <i>R</i> -3-MCHO/(643) | 6.76        | 8.08        | 69.1           | $6.8 \pm 0.1$ | $8.2 \pm 0.5$ | $64 \pm 3$   |
| Cyclohexanone/(1115)   | 6.76        | 6.76        | 85.9           | $6.7 \pm 0.1$ | $6.8 \pm 0.1$ | $84 \pm 1$   |
| Cyclohexanone/(532)    | 6.76        | 7.67        | 51.0           | $6.7 \pm 0.1$ | $7.7 \pm 0.1$ | $51 \pm 1$   |
| 2-hexanone/(643)       | 6.76        | 8.08        | 69.1           | $6.6 \pm 0.2$ | $8.0 \pm 0.4$ | $65 \pm 6$   |

<sup>a</sup> As illustrated in Fig. 1a and 2b,  $d_1$  is the kink–kink or adsorbate–adsorbate distance along the  $[\bar{1}3\bar{2}]$  step direction;  $d_2$  is the length of the other primitive vector for the corresponding surface structure or overlayer;  $\theta$  is the angle between the two primitive vectors.

Adsorbates with similar ring conformations, such as cyclohexane and cyclohexanone, both adopt similar orientation on Pt(111) [11] and graphite [12]. Such configurations maximize the van der Waals interaction between the molecule and the surface. Furthermore, we suggest that the ketone group is oriented toward kink sites, based on the known reactivity of such sites.

In previous TPD measurements of this system, molecular desorption peaks appeared with approximately equal intensities at 346 and 385 K following exposure of the *R*-Cu(643) surface to 3-MCHO at cryogenic temperatures [6,7]. In that study the two features in the TPD spectrum appearing above room temperature were ascribed to desorption of molecules adsorbed at step and kink sites, respectively. This picture was based upon the assumption of the roughening of step structure on the (643) surface, which in turn produces irregular kink spacing and substantially longer step edges that are free of kink sites. However, the present STM study indicates neither a significantly enhanced level of roughened step structure (Figs. 1b and 2a) nor the appearance of distinctly different adsorption sites for 3-*R*-MCHO following room temperature adsorption. As adsorption conditions have been observed to influence overlayer structures, we have attempted to explore the potential influence of surface temperature through additional measurements. In addition to the procedure described above, we dosed *R*-3-MCHO onto the

Cu(643) surface held at 90 K, and then warmed the sample to room temperature at a rate of  $\sim 1$  K/s. We found that the adsorption structure dosed at low temperature to be identical to that of the structure resulting from room temperature exposure and described above. One possible explanation of this apparent discrepancy can be found in the kinetic underpinnings of the TPD measurement. In such experiments, ‘peaks’ appear in the spectra as a result of simultaneously increasing desorption rates and decreasing surface coverages with increasing temperature. With this understanding, it can be seen that any temperature at which intensity in the spectrum is measured will lead to the complete desorption of the species, when allowing the system to reach equilibrium at this temperature. As such, it is possible that the leading edge of the 346 K peak extends below room temperature and neither of the STM experiments described above would capture this feature. Additional experiments are currently underway in which the adsorption structures of *R*-3-MCHO on Cu(643) are being explored at cryogenic temperatures.

### 3.3. Adsorption of cyclohexanone and 2-hexanone on Cu(643)

In order to investigate the influence of molecular structure on adsorption properties, we also studied the adsorption of cyclohexanone and 2-hexanone on Cu(643). As

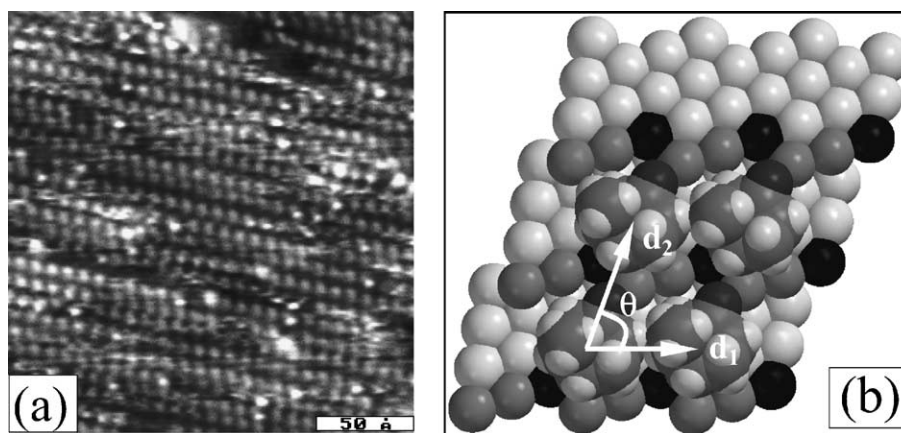


Fig. 2. (a) STM image of *R*-3-MCHO on Cu(643) as deposited at room temperature from an exposure of  $\sim 20$  L. The adsorption structure is very ordered along steps. Tunneling conditions:  $200 \text{ \AA} \times 200 \text{ \AA}$ ,  $-1.0$  V bias,  $0.7$  nA current. (b) Scaled model representation of the *R*-3-MCHO overlayer on Cu(643), illustrating the adsorption of one molecule per kink site.

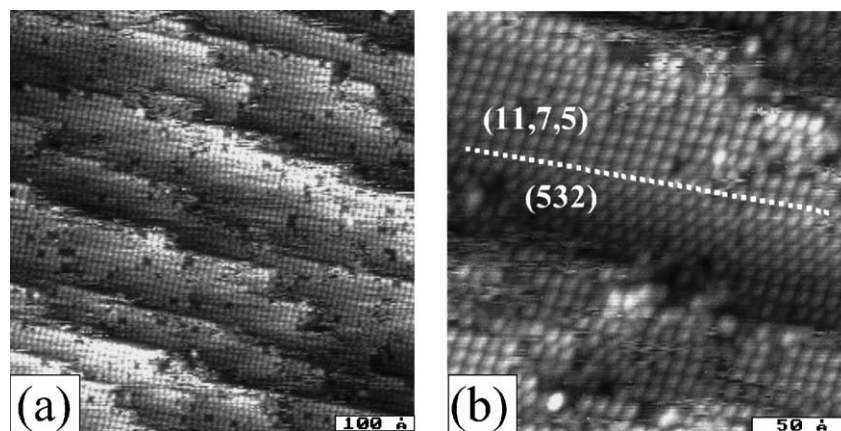


Fig. 3. STM images of cyclohexanone adsorbed on Cu(643) at room temperature from a  $\sim 20$ L exposure. Tunneling conditions: (a)  $500 \text{ \AA} \times 500 \text{ \AA}$ ,  $-1.0$  V bias,  $0.7$  nA current; (b)  $200 \text{ \AA} \times 200 \text{ \AA}$ ,  $-1.0$  V bias,  $0.7$  nA current. Analysis of the monolayer structure (Table 1) indicates the reconstruction of the underlying Cu(643) surface to (1175) (major) and (532) (minor) facets.

described in the following paragraphs, both ketones form ordered overlayers on the Cu(643) surface, however a surface reconstruction is detected in the case of cyclohexanone adsorption.

Although cyclohexanone possesses a ring structure and ketone functionality similar to *R*-3-MCHO, the adsorption of this molecule produces a different overlayer structure on Cu(643). The STM images in Fig. 3 illustrate the adsorption structure of cyclohexanone on Cu(643) formed from the room temperature exposure of  $\sim 20$ L. From the STM images, we find evidence for the restructuring of the Cu(643) surface, consistent with the formation of (1175) (major) and (532) (minor) facets (Fig. 4). These facets underlie the belt-like structures running across the image along the step direction and their formation can be viewed in terms of an effective reduction in terrace width while preserving the character of the step structure. The average width of the facets is  $\sim 70 \text{ \AA}$ . The domains associated with these facets are most clearly identified by differences in adsorbate–adsorbate spacing. Along the step direction, this spacing ( $d_1$ ) is  $6.7 \pm 0.1 \text{ \AA}$ , equivalent to that observed for

*R*-3-MCHO and the expected kink–kink distance of the ideal Cu(643) surface. However the spacing of adsorbate features appearing on separate terraces ( $d_2$ ) differs from the case of *R*-3-MCHO (Table 1). The models of (1175) and (532) surfaces shown in Fig. 4 are consistent with the measured dimensions of the terrace spacings in the different domains of the overlayer structure. From Fig. 3 we conclude that the reconstruction of the (643) surface accommodates the reduction of terrace width on a somewhat periodic basis through the formation of intermediate regions of wider terraces between the facets (consistent with the intermediate regions with fewer adsorbed molecules). We propose that the order overlayer structure is composed of cyclohexanone molecules existing in adsorption geometries similar to those of *R*-3-MCHO, primarily associated with the kink sites, however with the relatively smaller size of the cyclohexanone leading to the stabilization of more narrow terraces on the reconstructed surface.

In contrast, Fig. 5, displaying an STM image of the Cu(643) surface following room temperature exposure at  $\sim 20$ L of 2-hexanone, indicates the formation of ordered

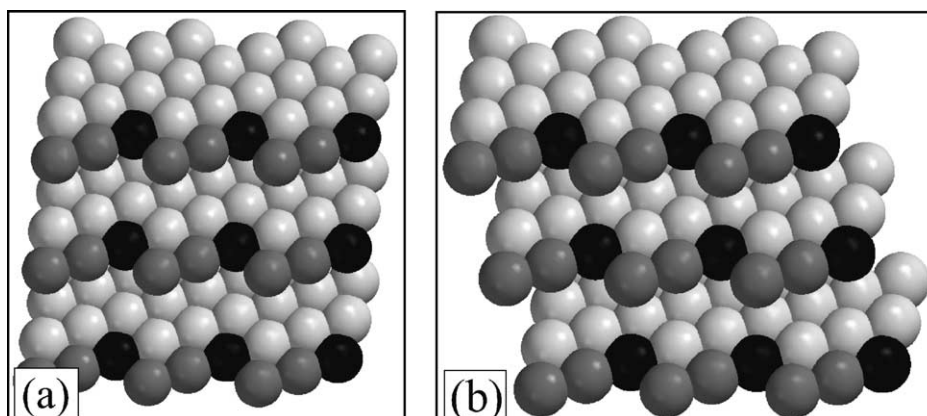


Fig. 4. Model structure of (a) Cu(1175) and (b) Cu(532). While the terrace width is reduced relative to the (643) surface, the reconstructed facets exhibit similar kinked step structures.

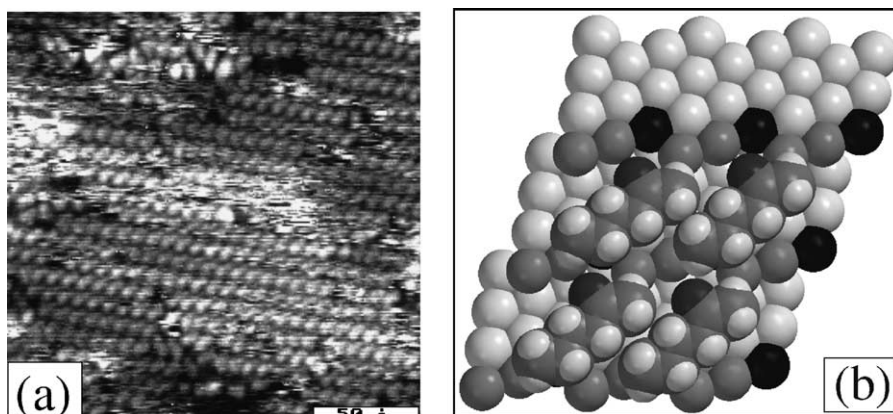


Fig. 5. (a) STM image obtained from Cu(643) surface exposed to  $\sim 20$  L 2-hexanone at room temperature obtained under the conditions:  $200 \text{ \AA} \times 200 \text{ \AA}$ ,  $-1.0$  V bias,  $0.7$  nA current. (b) Scaled model representation of 2-hexanone adsorbed on Cu(643).

overlayers identical to those formed from the adsorption of *R*-3-MCHO. In these images, the adsorbate–adsorbate spacing ( $d_1$ ) along the step direction again is  $6.6 \pm 0.2 \text{ \AA}$ , again equivalent to the kink–kink distance for the ideal Cu(643) surface. In contrast to the case for cyclohexanone adsorption, the spacing of molecular features on neighboring terraces ( $d_2$ ) following 2-hexanone adsorption is  $8.2 \pm 0.4 \text{ \AA}$ , similar to that observed for the clean Cu(643) surface and following adsorption of *R*-3-MCHO. Based on the orientation of the oblong molecular features in the STM images of the 2-hexanone overlayer structure, we propose that the chains exist in an all-*trans* extended conformation, lying parallel to the surface. As before, we consider the most reasonable adsorption geometry to entail the orientation of the ketone functionality towards the kink site.

#### 3.4. The role of molecular structure in adsorption

The STM data presented in this work demonstrates the high affinity of small ketones towards adsorption at the kink sites of vicinal copper surfaces. Through a comparison of ketones with different molecular structures, we have also demonstrated an apparent influence of molecular structure on the stability of vicinal copper surfaces in the following way. Molecular scale models of the overlayer structures described above clearly illustrate that the size of these adsorbates are of approximately the same dimension as the terrace widths. Furthermore, the STM data regarding cyclohexanone adsorption portrays the presence of a surface reconstruction involving the formation of a set of predominant terraces with reduced width, separated by small regions of increased terrace width. As cyclohexanone differs from *R*-3-MCHO and 2-hexanone primarily in its effective size, we propose that the vicinal copper surface is stabilized through the complete coverage of the terrace by adsorbates.

While these studies have not directly revealed the origin of the chiral activity, previously reported for the interaction of *R*-3-MCHO, they have identified several important issues to be considered in further exploring the nature of adsorption on chiral surfaces. First, these studies demonstrate the

ordered nature of steps and terraces of single-crystal, chiral metal surfaces. Second, the data presented here demonstrate the high mobility of metal atoms on the chiral surface and the possibility of facile surface reconstructions as a result of molecular adsorption. Finally, the data demonstrate the possibility of templating specific structures through the control of the molecular geometry and composition of adsorbates.

#### 4. Summary

Based upon the STM investigations presented in this paper, we find that the clean Cu(643) surface is well described by an ordered step and terrace structure containing single atom step heights. On the Cu(643) surface, the STM data indicate the high mobility of atoms at step edges in these room temperature measurements. In addition, the data portray that *R*-3-MCHO and 2-hexanone form similar ordered adsorption structures on Cu(643) at room temperature, with the molecular spacing commensurate with the ideal kink spacing of the underlying step structure. In contrast, cyclohexanone adsorption on Cu(643) induces a surface reconstruction entailing the formation of (1175) and (532) facets. These results collectively demonstrate a number of local surface phenomena that must be considered in describing adsorption on chiral surfaces.

#### Acknowledgements

The work has been supported by funds provided by the National Science Foundation (CMS-9876042). We are grateful to D. Sholl and A. Gellman for helpful discussions during the course of this study.

#### References

- [1] D.S. Sholl, A. Asthagiri, T.D. Power, J. Phys. Chem. B 105 (2001) 4771.

- [2] D.S. Sholl, *Langmuir* 14 (1998) 862.
- [3] T.D. Power, A. Asthagiri, D.S. Sholl, *Langmuir* 18 (2002) 3737.
- [4] A. Ahmadi, G. Attard, *Langmuir* 15 (1999) 2420.
- [5] G.A. Attard, C. Harris, E. Herrero, J. Feliu, *Faraday Discuss.* 121 (2002) 253.
- [6] J.D. Horvath, A.J. Gellman, *J. Am. Chem. Soc.* 124 (2002) 2384.
- [7] A.J. Gellman, J.D. Horvath, M.D. Buelow, *J. Mol. Catal. A* 167 (2001) 3.
- [8] M. Giesen-Seiber, F. Schmitz, R. Jentjens, H. Ibach, *Surf. Sci.* 329 (1985) 47.
- [9] J.C. Grard, S. Gauthier, S. Rousset, W. Sacks, S. de Cheveigné, J. Klein, *Surf. Sci.* 301 (1994) 245.
- [10] M. Giesen, *Surf. Sci.* 376 (1997) 55.
- [11] D.P. Land, W. Erley, H. Ibach, *Surf. Sci.* 289 (1993) 237.
- [12] M. Getzlaff, G. Schonhense, *Surf. Sci.* 377 (1997) 187.